9. R. Grantab, V. B. Shenoy, R. S. Ruoff, *Science* **330**, 946 (2010).
10. O. V. Yazyev, S. G. Louie, *Phys. Rev. B* **81**, 195420 (2010).
11. E. Cockayne et al., *Phys. Rev. B* **83**, 195425 (2011).
12. B. W. Jeong, J. Ihm, G.-D. Lee, *Phys. Rev. B* **78**, 165403 (2008).
13. J. H. Warner, N. P. Young, A. I. Kirkland, G. A. D. Briggs, *Nat. Mater.* **10**, 958 (2011).
14. O. L. Krivanek et al., *Nature* **464**, 571 (2010).
15. K. Suenaga, M. Koshino, *Nature* **468**, 1088 (2010).
16. J. Kotakoski, A. V. Krasheninnikov, U. Kaiser, J. C. Meyer, *Phys. Rev. Lett.* **106**, 105505 (2011).
17. J. C. Meyer et al., *Nat. Mater.* **10**, 209 (2011).
18. P. Y. Huang et al., *Nature* **469**, 389 (2011).
19. A. Hashimoto, K. Suenaga, A. Gloter, K. Urita, S. Iijima, *Nature* **430**, 870 (2004).
20. F. Banhart, J. Kotakoski, A. V. Krasheninnikov, *ACS Nano* **5**, 26 (2011).
21. B. Kabius et al., *J. Electron Microsc. (Tokyo)* **58**, 147 (2009).
22. M. Haider, P. Hartel, H. Müller, S. Uhlemann, J. Zach, *Microsc. Microanal.* **16**, 393 (2010).
23. M. Mukai et al., *Microsc. Microanal.* **11**, 2134 (2005).
24. J. C. Meyer et al., *Nano Lett.* **8**, 3582 (2008).
25. J. H. Warner et al., *Nat. Nanotechnol.* **4**, 500 (2009).
26. Z. Liu, K. Suenaga, P. J. F. Harris, S. Iijima, *Phys. Rev. Lett.* **102**, 015501 (2009).
27. J. R. Jinschek, E. Yucelen, H. A. Calderon, B. Freitag, *Carbon* **49**, 556 (2011).
28. X. Li et al., *Science* **324**, 1312 (2009).
29. A. W. Robertson et al., *ACS Nano* **5**, 6610 (2011).
30. C. Gómez-Navarro et al., *Nano Lett.* **10**, 1144 (2010).
31. M. J. Hÿtch, E. Snoeck, R. Kilaas, *Ultramicroscopy* **74**, 131 (1998).
32. Y. Kim, J. Ihm, E. Yoon, G.-D. Lee, *Phys. Rev. B* **84**, 075445 (2011).
33. F. Ding, K. Jiao, Y. Lin, B. I. Yakobson, *Nano Lett.* **7**, 681 (2007).

A Reduced Organic Carbon Component in Martian Basalts

A. Steele,[1]* F. M. McCubbin,[1,2] M. Fries,[3] L. Kater,[4] N. Z. Boctor,[1] M. L. Fogel,[1] P. G. Conrad,[5] M. Glamoclija,[1] M. Spencer,[6] A. L. Morrow,[6] M. R. Hammond,[6] R. N. Zare,[6] E. P. Vicenzi,[7] S. Siljeström,[8,9] R. Bowden,[1] C. D. K. Herd,[10] B. O. Mysen,[1] S. B. Shirey,[11] H. E. F. Amundsen,[12] A. H. Treiman,[13] E. S. Bullock,[14] A. J. T. Jull[15]

The source and nature of carbon on Mars have been a subject of intense speculation. We report the results of confocal Raman imaging spectroscopy on 11 martian meteorites, spanning about 4.2 billion years of martian history. Ten of the meteorites contain abiotic macromolecular carbon (MMC) phases detected in association with small oxide grains included within high-temperature minerals. Polycyclic aromatic hydrocarbons were detected along with MMC phases in Dar al Gani 476. The association of organic carbon within magmatic minerals indicates that martian magmas favored precipitation of reduced carbon species during crystallization. The ubiquitous distribution of abiotic organic carbon in martian igneous rocks is important for understanding the martian carbon cycle and has implications for future missions to detect possible past martian life.

Organic carbon in macromolecular reduced form has been detected in several martian meteorites, but there is little agreement on its provenance on Mars. Hypotheses for its origin include terrestrial contamination (*1*, *2*), chondritic meteoritic input (*3*), thermal decomposition of carbonate minerals (*4–6*), direct precipitation from aqueous fluids (*4*), and the remains of ancient biota (*7*). Confirming the presence and understanding the source and formation of this reduced carbon has implications for the carbon budget of Mars, its putative carbon cycle, carbon availability for biotic chemistry, life detection, and how to detect organic compounds on future Mars missions.

Eleven martian meteorites, including samples of the recent Tissint meteorite fall, were studied with confocal Raman imaging spectroscopy (CRIS). Macromolecular carbon (MMC) was identified in 10 of these meteorites associated with small (2 to 20 μm) metal oxide grains (hereafter referred to as spinel or oxide) that are ubiquitous as inclusions within olivine and/or pyroxene grains (Fig. 1 and fig. S1) (*8*). All of the MMC that we report here was located at least several microns below the top surface of the thin sections we analyzed (Fig. 1). The association of MMC with spinel is observed in recent falls (Tissint and Zagami), as well as older finds (DaG 476 and SAU 019) (table S1), making it unlikely to be terrestrial contamination (*9*).

MMC is characterized by the diagnostic disordered "D" Raman peak at ~1350 and the graphitic ordered peak at ~1590 cm^{-1} (Fig. 2, A and B) (*10*, *11*). MMC was initially detected within olivine-hosted melt inclusions in DaG 476 in association with oxide and pyroxene (table S1). DaG 476 is an olivine-phyric shergottite with olivine comprising 15 to 17% of the mode (fig. S1, A to E) (*12*). The oxides are fine-grained spinel-group minerals that appear to be magnetite or chromite based on the Raman peak positions. They are distributed throughout the olivine with enough grains below the surface to allow study of associated MMC that is completely encased within a silicate host (Fig. 1, A to F). With a combination of transmitted and reflected light, we determined the distance from the oxides to the surface and confirmed their isolation from any visible cracks (Fig. 1G). Figure 1G shows a three-dimensional (3D) CRIS depth profile of MMC occurring with spinel at a distance of 5 to 10 μm into the surface of DaG 476. Scanning electron microscopic (SEM) investigations of DaG 476 and SAU 130 showed oxides containing a carbon film that is texturally and chemically consistent with the MMC observed by CRIS (fig. S3) and is neither carbonate nor terrestrial microbial contamination (*12–14*).

Transmitted-light microscopy images and CRIS peak maps of a number of oxide grains hosted by pyroxenes in ALH 84001 and olivines from northwest Africa (NWA) 1110 demonstrate the co-occurrence of MMC phases with oxides in other meteorites analyzed (Fig. 1, H and I). In the

[1]Geophysical Laboratory, Carnegie Institution of Washington, 5251 Broad Branch Road, NW, Washington, DC 20015, USA. [2]Institute of Meteoritics, Department of Earth and Planetary Sciences, University of New Mexico, Albuquerque, NM 87131, USA. [3]Planetary Science Institute, 1700 East Fort Lowell, Suite 106, Tucson, AZ 85719, USA. [4]Witec GmbH, Lise-Meitner-Strasse 6, D-89081, Ulm, Germany. [5]NASA Goddard Space Flight Centre, 8800 Greenbelt Road, Greenbelt, MD 20771, USA. [6]Department of Chemistry, Stanford University, Stanford, CA 94305, USA. [7]Museum Conservation Institute, Smithsonian Institution, 4210 Silver Hill Road, Suitland, MD 20746, USA. [8]Department of Geological Sciences, Stockholm University, 10691 Stockholm, Sweden. [9]Department of Chemistry and Materials, SP Technical Research Institute of Sweden, 501 15 Borås, Sweden. [10]Department of Earth and Atmospheric Sciences, University of Alberta, Edmonton, AB T6G 2E3, Canada. [11]Department of Terrestrial Magnetism, Carnegie Institution of Washington, 5241 Broad Branch Road, NW, Washington, DC 20015, USA. [12]Earth and Planetary Exploration Services, Jacob Aals Gate 44b, 0364 Oslo, Norway. [13]Lunar and Planetary Institute, 3600 Bay Area Boulevard, Houston, TX 77058, USA. [14]Department of Mineral Sciences, Smithsonian Institution, Washington, DC 20013–7012, USA. [15]University of Arizona, 1118 East Fourth Street, Tucson, AZ 85721, USA.

*To whom correspondence should be addressed. E-mail: asteele@ciw.edu

case of NWA 1110 (Fig. 1), the oxides are zoned with chromite cores and iron-rich (magnetite) rims, with MMC predominantly associated with the chromite phase. In general, two types of associations were observed: (i) pyroxene + oxide + MMC hosted in olivine and (ii) oxide + MMC hosted in pyroxene. Minor phases such as pyrrhotite and apatite are sometimes observed.

We have used the G-band peak center and full width at half maximum (FWHM) to indicate the maturity level and crystallinity of MMC (15, 16). The MMC data (Fig. 2B) show a large range of G-band peak shapes and on the whole are indicative of amorphous to poorly ordered graphitic carbon in the range recorded for carbonaceous chondrites and interplanetary dust particles (IDPs) (16). The MMC in Tissint and Zagami appears to have a higher degree of graphitic order than that seen in the other martian meteorites except NWA 1110. Within individual meteorites (i.e., ALH 84001 and DaG 476), there is substantial variation in the G-band parameters (Fig. 2B). This variation may indicate different formation conditions or mild heating after MMC formation.

To further elucidate the chemical composition of the amorphous to poorly ordered graphitic carbon measured by CRIS, we conducted laser desorption laser ionization mass spectrometry (L^2MS) analysis (17) on exposed olivine phenocrysts from a crushed sample of DaG 476 to identify any possible polycyclic aromatic hydrocarbons (PAHs) associated with the MMC (9). Compared with MMC extracted from a Murchison reference standard and several controls, DaG 476 contains a range of PAHs, including phenanthrene (and alkylated derivatives), pyrene, perylene, and anthracene similar to that seen in the Murchison meteorite (fig. S4). Apart from chrysene, the major PAH molecules observed are similar to those seen previously in ALH 84001 (7), although the degree of alkylation of phenanthrene is more pronounced in DaG 476. The degree of alkylation of phenanthrene has been used as an indicator of parent-body processing in carbonaceous chondrites and does not necessarily represent an indicator of biogenicity or contamination (7, 18). Substantial PAHs were not present on the surface of the samples or controls and were only detected when the inclusions were revealed after etching of the silicate minerals. Furthermore, the controls show that no PAHs were added to the samples during analysis (9). The lack of dibenzothiophene (184 atomic mass units), a ubiquitous contaminant associated with PAHs from terrestrial sources, also indicates that the PAHs measured were not terrestrial (7). Previous studies of the MMC of carbonaceous chondrites by L^2MS and CRIS show similar PAH distributions and Raman G-band parameters to those observed in the present study (18, 19). Thus, the PAHs found in DaG 476 must be indigenous to this meteorite and a component of the MMC detected by Raman spectroscopy. We expect that PAHs are a probable constituent of the MMC found in the other martian meteorites analyzed.

The presence of PAHs in the martian meteorites we studied is in accord with current models and observations documenting MMC and PAH synthesis over a diverse range of pressure and temperature conditions, including temperatures >3000 K in the solar nebula and 1400 K in industrial blast furnaces (20). The distribution of PAHs and MMC alone cannot distinguish whether the carbon was produced biologically or abiologically (21); thus, textural relationships between MMC and any coexisting mineral phases become paramount to determining the possible mechanism of formation and incorporation in crystallizing silicates. Because MMC was always associated with igneous phases, we conclude that it crystallized from the host magma. This textural relationship negates any biological origin of the MMC and PAHs.

We analyzed bulk samples of DaG 476, SAU 130, and Dhofar 019 for ^{14}C (table S1) (9) to determine the presence of a young (terrestrial) C component. The ^{14}C measurements suggest that although modern terrestrial carbon was present in all the meteorites, there was also a portion of organic carbon that is probably indigenous to Mars (9), which is consistent with previous results from Nakhla and ALH 84001 (1, 22, 23).

Fig. 1. (**A**) Transmitted-light image of a single inclusion 4 μm below the surface of DaG 476 (scale bar, 3 μm). (**B** to **F**) Raman maps of the same inclusion as (A) (the lighter the color, the more intense the mapped peak). (B) Olivine (~820 cm⁻¹), (C) pyroxene (~1005 cm⁻¹), (D) spinel-group oxide (~670 cm⁻¹), (E) MMC (carbon G-band 1580 cm⁻¹), (F) red-green-blue color image. Green, Px, pyroxene; red, Sp, spinel-group oxide; blue, MMC. White arrows show the joint occurrence of oxides and MMC. (**G**) A CRIS 3D depth profile through a melt inclusion 5 to 20 μm into the sample surface within DaG 476. Red, Sp, spinel-group oxide; blue, MMC (grid is in 2-μm increments). MMC is visualized as blue when in isolation and as purple when with oxides. (**H**) Raman peak images of peak center shift map of oxide from 660 to 720 cm⁻¹ (lighter orange, higher wave number, more chromite rich; darker orange, lower wave number, magnetite rich) in inclusions in NWA1110 (scale bar 7 μm). (**I**) Blue-green image of peak center shift map showing the occurrence of MMC with higher–wave number chromite-rich phase. Blue, MMC; green, spinel-group oxide. (**J**) Transmitted-light image of inclusions within pyroxenes in ALH 84001. Scale bar, 3 μm). (**K** and **L**) Raman peak maps of (K) spinel-group oxide and (L) MMC. Scale bars, 3 μm.
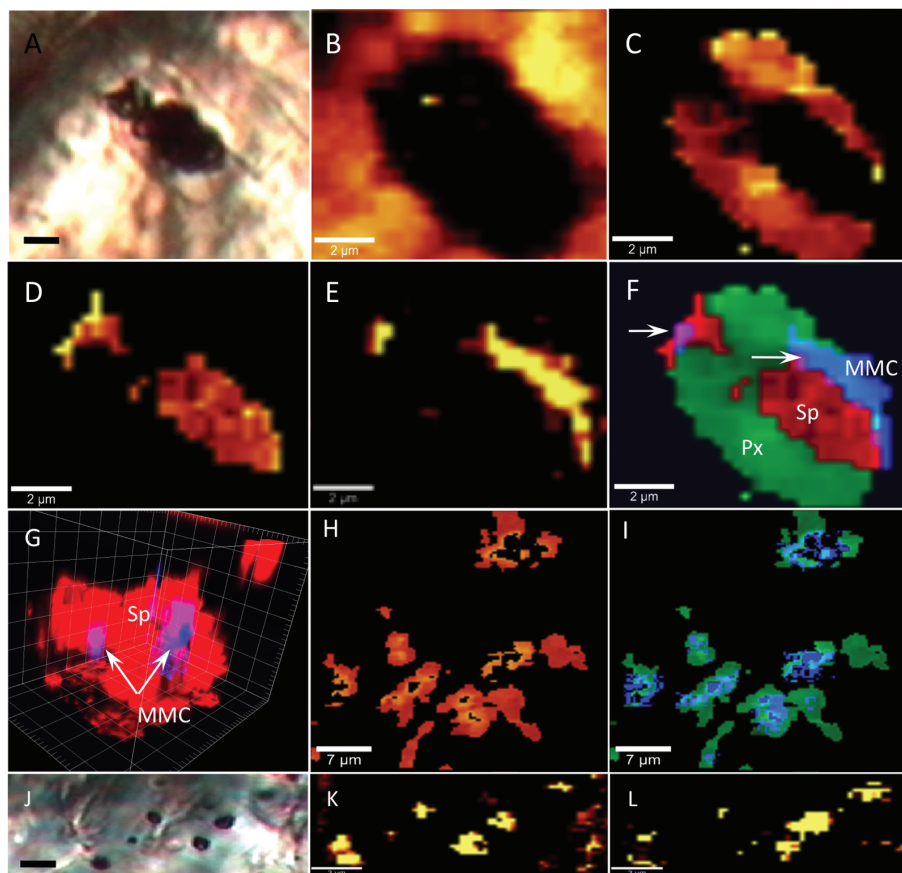
The stable carbon isotope compositions ($\delta^{13}C$) for Zagami, NWA 998, SaU 130, and DaG 476 are consistent with previous results of MMC in martian meteorites (24); however, our results averaged ~16 parts per million (ppm) C for the shergottites, about four times as much as previous results (24) (table S1). This difference is consistent for both falls and finds and may be due to differences in analytical techniques, interference from low levels of terrestrial contamination, or sample heterogeneity.

The Tissint meteorite, which fell in July 2011 in the Moroccan desert, represented a unique opportunity to study a minimally contaminated martian sample. It has 14 ppm of reduced C with a $\delta^{13}C$ of −17.8 ± 1.9 per mil (‰), similar to the other martian meteorites. The similarity of the C content and $\delta^{13}C$ of Tissint with the other martian meteorites and the presence of C without substantial ^{14}C supports the finding that much of its carbon is of martian origin. Combining ours and other studies, igneous martian rocks could contain an average of ~20 ± 6 ppm of reduced carbon with a $\delta^{13}C$ of ~ −19.8 ± 4.3‰. Grady et al., (24) speculated that the carbon they detected was along grain boundaries and within silicate inclusions. Our in situ and bulk investigations corroborate their findings and suggest that some of the carbon occurs as a PAH-containing MMC phase within mineral-hosted crystalline melt inclusions.

The MMC-bearing oxides are fully encapsulated in igneous crystals of olivine and/or pyroxene, suggesting that such oxides are also igneous in origin. Inclusions consisting primarily of oxide (+MMC) are likely microphenocrysts encapsulated by the growing silicate crystals, whereas multiphase inclusions represent melt inclusions with oxide microphenocrysts (Fig. 3). The disordered nature of the MMC and the presence of PAHs in the MMC-containing assemblages indicate that the MMC precipitated in contact with the oxides as an insoluble organic
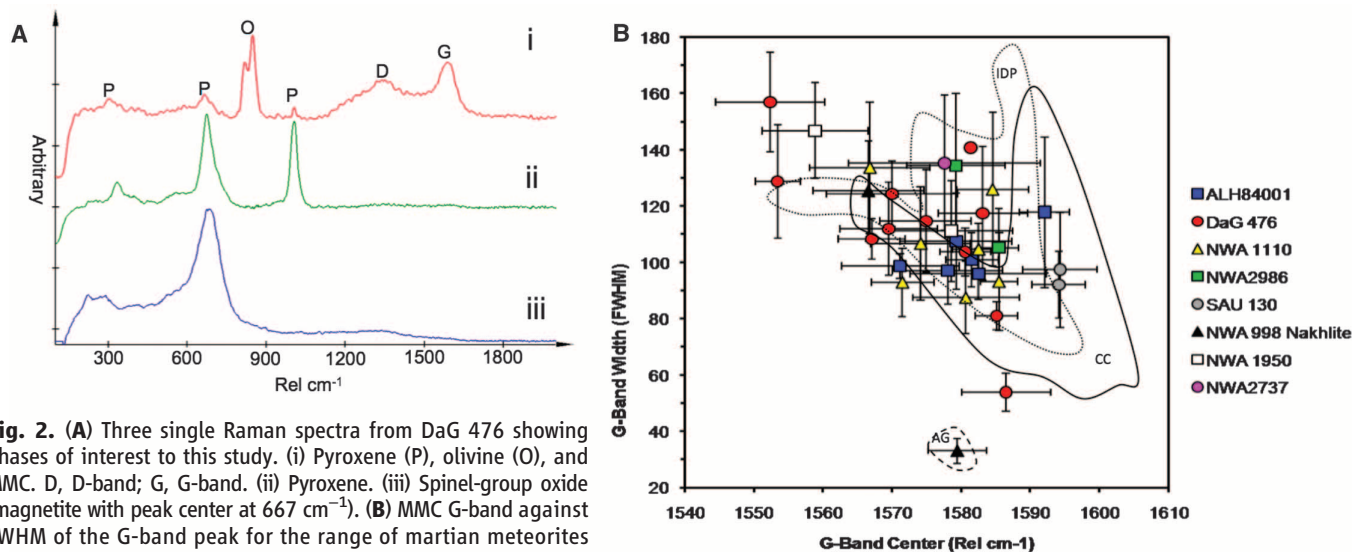
Fig. 2. (A) Three single Raman spectra from DaG 476 showing phases of interest to this study. (i) Pyroxene (P), olivine (O), and MMC. D, D-band; G, G-band. (ii) Pyroxene. (iii) Spinel-group oxide (magnetite with peak center at 667 cm^{-1}). (B) MMC G-band against FWHM of the G-band peak for the range of martian meteorites in which MMC has been detected. The area bordered by a black line is the variation in these parameters observed in carbonaceous chondrites (CC); the area bordered by a dotted black line shows the parameters exhibited by interplanetary dust particles (IDP). AG is a standard spectrum of graphite and represents ordered crystalline carbon; disorder in the MMC increases with decreasing G-band center and increasing FWHM (19).

Fig. 3. Proposed crystallization sequence for the MMC-bearing melt inclusions along with a pressure-temperature schematic illustrating the process that correlates to each of the crystallization sequence panes [(A) to (D)]. (A) Trapping of liquid in olivine. (B) Ascent and cooling allow inclusion to begin to crystallize. (C) Continued crystallization of melt inclusion during cooling. (D) CRIS image of a trapped inclusion in olivine from DAG 476. Black arrows indicate the direction of the crystallization sequence. The depth of melting (1 to 3 GPa or 75 to 225 km depth) is within the pressure range of experimentally determined multiple saturation points for shergottites shown to be representative of liquid compositions [i.e., (26, 40)]. Phenocryst growth at higher pressure may take place at the base of the martian crust as it acts as a natural density barrier for melts to pond and begins to crystallize [as proposed by (41)].
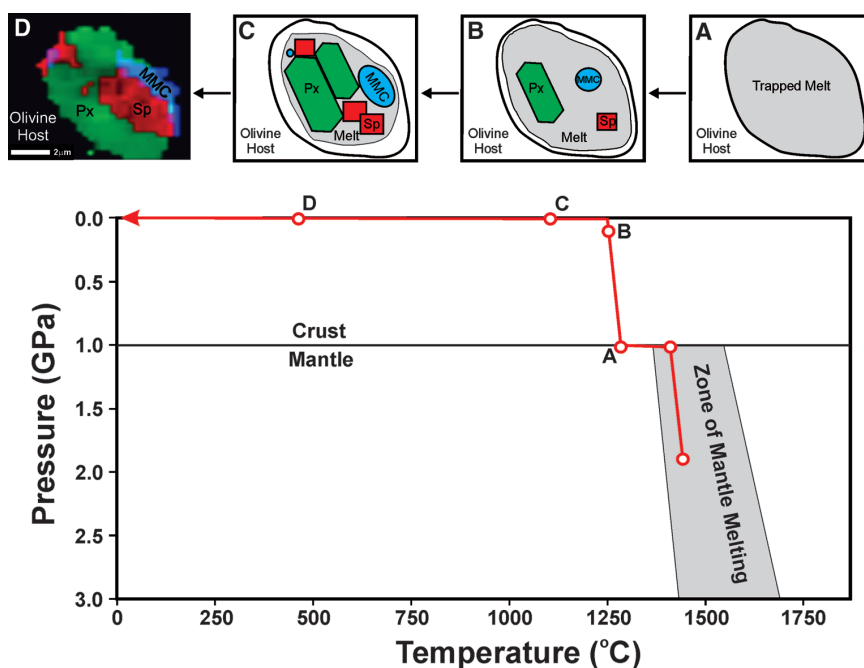
carbon phase that was sensitive to the redox state of the magma. It has been hypothesized that the martian mantle is saturated with respect to graphite and that the oxygen fugacities (f_{O_2}) of the mantle sources for the martian meteorites are buffered by fluids in the C-O-H system (*25*, *26*), consistent with f_{O_2} recorded by many of the martian meteorites (table S1) (*9*, *27–29*). Substantial amounts of hydrogen occur in martian magmatic source regions (*30*, *31*), indicating that if the martian mantle is graphite saturated, partial melts of the mantle would have contained substantial C-O-H components. Trapping of a C-O-H–bearing melt in the mineral host would have led to the early saturation in a graphite + C-O-H fluid-phase in the melt inclusion that would have increased in volume as the rock cooled and crystallized (Fig. 3). Importantly, C-O-H fluid + graphite is the structural equivalent of MMC, if the C-O-H fluid and graphite were to form a single phase. The formation of a single MMC phase is further supported by the lack of void space within the inclusions coupled with the absence of any gaseous species identified by CRIS (i.e., H_2O, CO_2, or CH_4) in the many hundreds of inclusions analyzed. This observation indicates that MMC formation was probably not by catalysis of volatiles with the oxide phases, unless this catalysis occurred while the volatile components were dissolved in the silicate melt. The formation mechanism that we propose for MMC production is supported by experimental data on the C-O-H system in which low f_{O_2} and high f_{H_2} conditions produced MMC and PAHs at 1000 K (*32*). In that study, formation of CH_4 and crystalline graphite were inhibited, allowing for the formation of MMC, including PAHs. The C:H ratio of the fluid changes the size and distribution of polycyclic aromatic species, and MMC may shift toward graphitic at low f_{H_2} and to very amorphous at higher f_{H_2}, explaining the MMC G-band parameter heterogeniety seen in our study (*32*) (Fig. 2B).

From the crystallization ages of these martian meteorites (table S1), it appears that some portion of the martian carbon budget has existed as MMC from at least 4.2 billion years ago to 190 million years ago (*33*, *34*). Hirschmann and Withers (*25*) postulated on the formation of a martian atmosphere from a reduced mantle and concluded that CO_2 degassing to the martian surface may have been severely limited. Our results confirm the presence of reduced MMC species in reduced (less than quartz-fayalite-magnetite) igneous rocks, and therefore support the central tenet of the Hirschmann and Withers (*25*) study. However, the lack of MMC in inclusions in the most oxidized sample (Nakhla) illustrates the possible effects of the redox state of the martian magmas on the preservation of these carbon species during crystallization. This, in turn, has an effect on their distribution at the surface and within the crust (*35*, *36*).

Our analyses did not detect CH_4 or CO_2 within any igneous inclusions. Methane detected in the atmosphere of Mars has been explained by both abiotic and biotic processes (*37*, *38*), although there is some doubt to its presence at all (*39*). Our data cannot prove a link between igneous processes and the presence of putative methane; however, the reduced conditions implied by the presence of MMC could affect carbon in the atmosphere on Mars tentatively supporting abiotic production of CH_4 (*37*, *38*). The youngest MMC-bearing meteorite (~190 million years old), demonstrates that reduced carbon phases have been generated recently in Mars' history and, therefore, that the martian reduced carbon budget was in flux during the late Amazonian, hinting that a true martian carbon cycle may still be active.

Our results imply that primary organic carbon is nearly ubiquitous in martian basaltic rocks. It formed through igneous, not biological, processes and was delivered over most of martian geologic history to the surface as recently as the late Amazonian. Therefore, a positive detection of organics (especially PAHs) on Mars by Mars Science Laboratory, even if coupled with isotopically "light" $\delta^{13}C$ values, may be detecting this abiotic reservoir. Furthermore, the origin of the carbon in mantle rocks is strong evidence that this carbon was indigenous to the martian interior because the absence of extensive plate tectonics would have prevented exchange between surface and near-surface carbon reservoirs (*9*). Consequently, the storage of carbon within Mars occurred very early in its history, at the time of planet-wide differentiation (*9*), which has also been suggested for hydrogen storage on Mars (*31*). This process is likely not unique to Mars and could have been widely responsible for the production and delivery of abiotic organic carbon to the surfaces of the other terrestrial planets, including early Earth.

References and Notes

1. A. J. T. Jull, C. Courtney, D. A. Jeffrey, J. W. Beck, *Science* **279**, 366 (1998).
2. T. Stephan, E. K. Jessberger, C. H. Heiss, D. Rost, *Meteorit. Planet. Sci.* **38**, 109 (2003).
3. L. Becker, B. Popp, T. Rust, J. L. Bada, *Earth Planet. Sci. Lett.* **167**, 71 (1999).
4. A. Steele et al., *Meteorit. Planet. Sci.* **42**, 1549 (2007).
5. A. H. Treiman, *Astrobiology* **3**, 369 (2003).
6. M. Y. Zolotov, E. L. Shock, *Meteorit. Planet. Sci.* **35**, 629 (2000).
7. D. S. McKay et al., *Science* **273**, 924 (1996).
8. Any MMC found to be incompletely enclosed within its silicate host (i.e., in cracks, grain boundaries, at the surface of the sample, or associated with weathering or contaminating phases) was treated as contamination and discounted from this study.
9. Materials, methods, and supporting text are available as supplementary materials on *Science* Online.
10. M. Fries, A. Steele, *Science* **320**, 91 (2008).
11. A. Steele et al., *Science* **329**, 51 (2010).
12. J. Zipfel, P. Scherer, B. Spettel, G. Dreibus, L. Schultz, *Meteorit. Planet. Sci.* **35**, 95 (2000).
13. A. Steele et al., *Meteorit. Planet. Sci.* **35**, 237 (2000).
14. J. Toporski, A. Steele, *Astrobiology* **7**, 389 (2007).
15. O. Beyssac, B. Goffe, C. Chopin, J. N. Rouzaud, *J. Metamorph. Geol.* **20**, 859 (2002).
16. G. D. Cody et al., *Earth Planet. Sci. Lett.* **272**, 446 (2008).
17. The detection sensitivity of the L^{2}MS technique is in the femtomolar range for PAHs.
18. S. Messenger et al., *Astrophys. J.* **502**, 284 (1998).
19. S. A. Sandford et al., *Science* **314**, 1720 (2006).
20. M. Y. Zolotov, E. L. Shock, *J. Geophys. Res. Solid Earth* **105**, 539 (2000).
21. J. D. Pasteris, B. Wopenka, *Astrobiology* **3**, 727 (2003).
22. A. J. T. Jull, J. W. Beck, G. S. Burr, *Geochim. Cosmochim. Acta* **64**, 3763 (2000).
23. A. J. T. Jull, in *Meteorites and the Early Solar System II*, D. S. Lauretta, H. Y. McSween Jr., Eds. (Univ. of Arizona Press, Tucson, AZ, 2006), pp. 889–905.
24. M. M. Grady, A. B. Verchovsky, I. P. Wright, *Int. J. Astrobiol.* **3**, 117 (2004).
25. M. M. Hirschmann, A. C. Withers, *Earth Planet. Sci. Lett.* **270**, 147 (2008).
26. K. Righter, H. Yang, G. Costin, R. T. Downs, *Meteorit. Planet. Sci.* **43**, 1709 (2008).
27. C. D. K. Herd, *Meteorit. Planet. Sci.* **38**, 1793 (2003).
28. M. Wadhwa, *Rev. Mineral. Geochem.* **68**, 493 (2008).
29. M. Wadhwa, *Science* **291**, 1527 (2001).
30. F. M. McCubbin et al., *Earth Planet. Sci. Lett.* **292**, 132 (2010).
31. F. M. McCubbin et al., *Proc. 43rd Lunar Planet. Sci. Conf.* **43**, 1121 (2012).
32. R. V. Eck, E. R. Lippincott, M. O. Dayhoff, Y. T. Pratt, *Science* **153**, 628 (1966).
33. L. E. Borg, D. S. Draper, *Meteorit. Planet. Sci.* **38**, 1713 (2003).
34. T. J. Lapen et al., *Science* **328**, 347 (2010).
35. R. V. Morris et al., *Science* **329**, 421 (2010).
36. J. R. Michalski, P. B. Niles, *Nat. Geosci.* **3**, 751 (2010).
37. S. K. Atreya, P. R. Mahaffy, A. S. Wong, *Planet. Space Sci.* **55**, 358 (2007).
38. M. J. Mumma et al., *Science* **323**, 1041 (2009).
39. K. Zahnle, R. S. Freedman, D. C. Catling, *Icarus* **212**, 493 (2011).
40. D. S. Musselwhite, H. A. Dalton, W. S. Kiefer, A. H. Treiman, *Meteorit. Planet. Sci.* **41**, 1271 (2006).
41. F. M. McCubbin, H. Nekvasil, A. D. Harrington, S. M. Elardo, D. H. Lindsley, *J. Geophys. Res. Planets* **113**, (E11), E11013 (2008).

Science

A Reduced Organic Carbon Component in Martian Basalts

A. Steele, F. M. McCubbin, M. Fries, L. Kater, N. Z. Boctor, M. L. Fogel, P. G. Conrad, M. Glamoclija, M. Spencer, A. L. Morrow, M. R. Hammond, R. N. Zare, E. P. Vicenzi, S. Siljeström, R. Bowden, C. D. K. Herd, B. O. Mysen, S. B. Shirey, H. E. F. Amundsen, A. H. Treiman, E. S. Bullock and A. J. T. Jull

Abiotic Martian Organics

Understanding the sources and the formation mechanisms of organic carbon compounds on Mars has implications for our understanding of the martian carbon cycle. **Steele** *et al.* (p. 212, published online 24 May) present measurements of organic material in 11 martian meteorites, including the Tissint meteorite, which fell in the Moroccan desert in July 2011. Ten of the meteorites contain complex hydrocarbons encased within igneous minerals. The results imply that the organics formed as the magma melt crystallized and are thus of abiotic origin.

ARTICLE TOOLS	http://science.sciencemag.org/content/337/6091/212
SUPPLEMENTARY MATERIALS	http://science.sciencemag.org/content/suppl/2012/05/23/science.1220715.DC1
RELATED CONTENT	http://science.sciencemag.org/content/sci/336/6084/970.full file:/contentpending:yes
REFERENCES	This article cites 65 articles, 17 of which you can access for free http://science.sciencemag.org/content/337/6091/212#BIBL
PERMISSIONS	http://www.sciencemag.org/help/reprints-and-permissions